

## Atmospheric Excitation of Polar Motion

David Salstein

*Atmospheric and Environmental Research, Inc., 840 Memorial Drive,  
Cambridge, MA 02139 USA*

**Abstract.** Variations in the angular momentum of the atmosphere in the equatorial plane due to shifts in air mass distribution and changing winds impact the orientation of Earth so that motions of the pole occur on a broad range of time scales. The wind terms have notable diurnal fluctuations, which appear as a tidal signature. Subseasonal fluctuations of the pole are shown to be related to the atmospheric signal on scales as short as at least a week, according to a coherency analysis. Atmospheric mass fluctuations over certain regions, such as Eurasia and North America, appear to be more responsible for rapid polar motions than are those elsewhere, and may be related to known climate modes. On the other hand, atmospheric pressure fluctuations over the ocean are counteracted in large measure by a sea level response, due to an inverted barometer relationship. Ocean forcing from model results assist in narrowing the differences in the geodetic and atmospheric budgets. Efforts to assess dynamic forecasts of the atmospheric polar motion excitations have demonstrated positive skill out to at least 10 days for the mass term.

### 1. Introduction

The Earth can be viewed as a system in which angular momentum, a vector quantity, is conserved (Barnes *et al.* 1983). The variations of this angular momentum within one terrestrial component therefore affect those in the others. Changes in atmospheric angular momentum about the two axes in the equatorial plane, impacting the motions of the pole, arise either from shifts in the air mass distribution or from varying winds. Those changes occurring about the axis of rotation are related to fluctuations in the rate of rotation, influencing changes in the length of day. In the axial length-of-day case, the largely axisymmetric wind fluctuations are the dominant agent for this type of interaction, but the opposite is the case for polar motion. Redistribution of atmospheric mass, noted as changes in surface pressure, has a stronger effect than the winds on most time scales, as related to polar motion. Polar motions have been shown to be related to the atmosphere on subseasonal timescales as short as about one week. The atmospheric excitations are being monitored by the Special Bureau for the Atmosphere (SBA; formerly the Sub-bureau for Atmospheric Angular Momentum; Salstein *et al.* 1993) of the International Earth Rotation Service. Comparisons between centers have helped determine uncertainties in the excitation numbers

themselves. Signals in the subdiurnal band, due in part to a tidal signature in atmospheric winds, show specific distinctions between the centers.

We will review the types of atmospheric fluctuations responsible for polar motion, and discuss the locations at which the most important fluctuations occur in this context. Because the atmosphere also interacts with the oceans below, the two bodies also have an interplay exciting polar motion. We note that pressure excitation may be modified with the inclusion of the “Inverted Barometer” approximation, in which the atmospheric mass fluctuations over the atmosphere are compensated in large measure by those in the underlying ocean (Ponte *et al.* 1991). The ocean’s mass and velocity fluctuations themselves also contribute to polar motion excitation, and this relationship is discussed in later sections.

Forecasts of the atmospheric excitation terms for polar motion are calculated by the SBA and their utility is being assessed. Based on the winds and surface pressures emerging from the same models that perform weather forecasts, these forecasted quantities generally show skill out to lead times of 10 days. Results are reviewed later.

## 2. Excitation terms for polar motion

The atmospheric terms related to the polar motion component towards 0 and 90E longitudes, from the wind (W) and pressure (P) components, expressed below in the Barnes *et al.* (1983) formulation, are the basis for the calculations at the SBA.

$$\begin{aligned}\chi_1^p &= \frac{-1.00R^4}{(C-A)g} \iint p_s \sin \phi \sin^2 \phi \cos \lambda d\lambda d\phi, \\ \chi_1^w &= \frac{-1.43R^3}{W(C-A)g} \iiint (u \sin \phi \cos \phi \cos \lambda - v \cos \phi \sin \lambda) d\lambda d\phi dp, \\ \chi_2^p &= \frac{-1.00R^4}{(C-A)g} \iint p_s \sin \phi \cos^2 \phi \sin \lambda d\lambda d\phi, \\ \chi_2^w &= \frac{-1.43R^3}{W(C-A)g} \iiint (u \sin \phi \cos \phi \sin \lambda + v \cos \phi \cos \lambda) d\lambda d\phi dp.\end{aligned}$$

Here  $R$  is radius of the Earth,  $C$  and  $A$  are Earth’s axial and equatorial moments of inertia,  $W$  is Earth’s mean rotation rate,  $g$  is mean acceleration of gravity,  $u$  and  $v$  are zonal and meridional winds, with eastward and northward directions respectively positive,  $\phi$  latitude,  $\lambda$  longitude,  $p$  pressure, and  $p_s$  surface pressure. A sample of polar motion excitation from the National Center for Environmental Prediction (NCEP) is shown in Fig. 1 for wind, pressure and pressure as modified by the Inverted Barometer formulation, given 4 times per day for 1998, the most recent full year. Eliminating the diurnal fluctuations in the wind terms by taking the daily average (dark curve) much reduces the power in the series. The pressure-related terms (whose diurnal averages are essentially the same as the plot) dominate the variance of the polar motion excitation (longer than one day), though applying the IB model reduces that contribution.

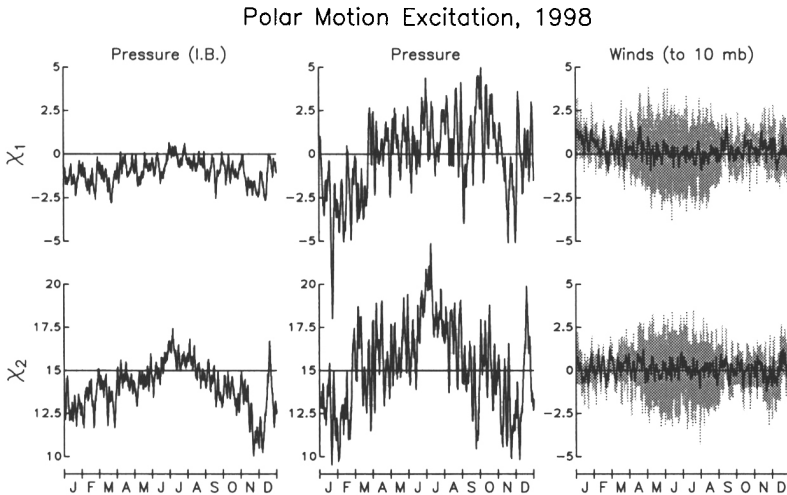


Figure 1. Excitations during 1988 of the two components of polar motion, for the pressure term (4 times per day), both accounting for the inverted barometer (IB) term, and not accounting for it, and for the wind component (4 times per day in grey, daily average, in black). Units are non-dimensional times  $10^{-7}$ .

Four operational centers (see table below) participate in the SBA, transferring polar motion excitation values from atmospheric analyses and forecasts, along with other related data of geodetic importance. These values are available on a near-real time basis for at least the previous ten days, and their whole history is in the archives of the SBA. Because operational data were characteristic of the specific system in use at the time of their production, some meteorological centers decided to reanalyze the data using a consistent modern set. The SBA calculates the polar motion excitation functions from three of these centers. Information regarding the 7 data sets thus produced is given in Table 1.

Polar motion at subseasonal scales is strongly, though not completely related to atmospheric forcing. We see, for example, in the results for 1998 (Fig. 2), that the correlation between the pressure plus wind with polar motion excitation terms are 0.48 and 0.75. When the pressure (IB) term is used instead of the pressure without IB, the correlation increases to 0.70 and 0.84, for the  $\chi_1$  and  $\chi_2$  components, respectively agreeing with the overall sense of the coherence results in this band in Fig. 3. A spectrum of polar motion excitations for the P-IB plus W terms versus the actual polar motion excitation function (one component, to give an example) shows the relationship by frequency (Fig. 4), revealing that the power is generally consistent in the two series. However, there is insufficient power in the atmosphere to force polar motion in the band between about 8 and 30 days. For the higher frequencies the atmosphere is stronger than the geodetic series (IERS EOPC04) which is smoothed in these frequencies; other solutions in fact give a difference with the opposite sign.

Table 1. Datasets in the SBA.

Operational Center	Top level (hPa)	Period of record	Max forecast lead (current/past)
U.S. National Centers for Environmental Prediction (NCEP)	10	1976–	5 days / 10 days
United Kingdom Meteorological Office (UKMO)	25	1987–	6 days
Japan Meteorological Agency (JMA)	10	1993–	8 days
European Centre for Medium-Range Weather Forecasts (ECMWF)	10	1988	7 days

Reanalysis Center	Top level (hPa)	Period of record
National Centers for Environmental Prediction/National Center for Atmospheric Research	10	1948–
European Centre for Medium-Range Weather Forecasts	10	1979–93
NASA Goddard Laboratory for Atmospheres	20	1980–95

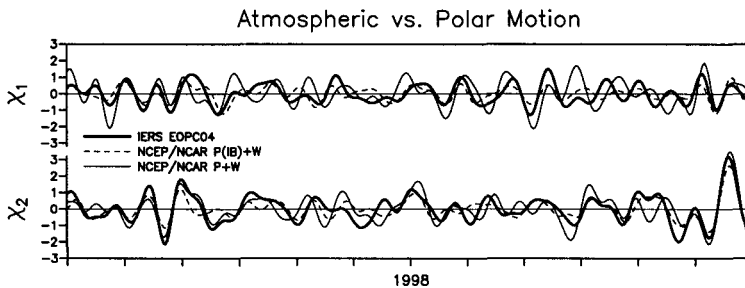


Figure 2. A comparison of atmospheric (including or not including the IB effect) and geodetic excitations for polar motion, filtered between 14 and 40 days for the year 1988. Units are non-dimensional times  $10^{-7}$ .

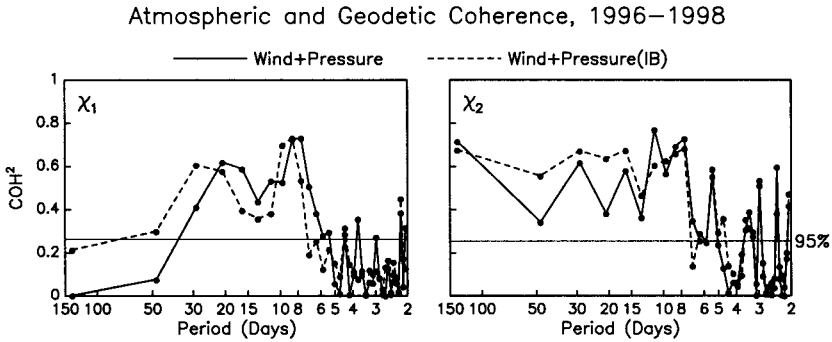


Figure 3. Coherence between geodetic and atmospheric terms (including or not including the IB effect) between 2 and 150 days. The horizontal line gives the measure of 95% significance.

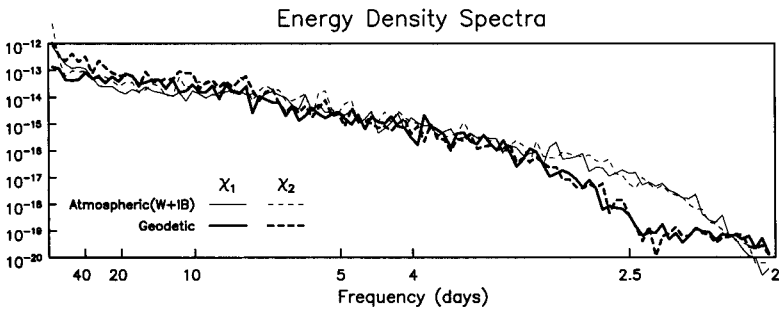


Figure 4. Power spectrum of atmospheric and geodetic excitation terms for 1996–1998.

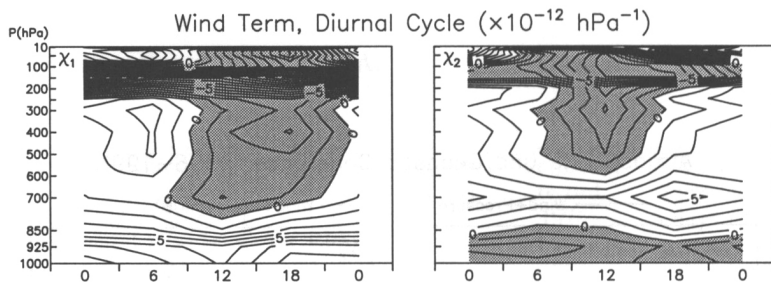


Figure 5. Mean diurnal cycle of wind-based atmospheric excitations of polar motion, during July 1999 based on 4 synoptic hours.

### 3. Diurnal band of polar motion excitation

When the wind terms for polar motion are separated into each of four synoptic hours, the tidal responses of model/analysis systems are revealed (Bell 1994). The largest such response occurs during the Northern Hemisphere summer, when heating from the northern continents is at its maximum. During that season, convergence and divergence in wind patterns in the lower and upper atmosphere have a strong diurnal signature (Hsu & Hoskins 1989). This diurnal signature projects strongly onto the two wind excitation values. When the values for a summer month (July 1999) are averaged separately at each of the four available synoptic hours (00, 06, 12, and 18 UT), they form a diurnal signal whose  $\chi_1$  and  $\chi_2$  maxima are at 06 and 00 UT, respectively. Such a signal is captured by at least three of the analysis sets that resolve the four times daily signals (NCEP, ECMWF, NCEP/NCAR reanalyses). When the contributing wind fields are analyzed by level, the mean wind-based excitation fields show their strongest diurnal cycle in the middle and upper troposphere and in the stratosphere (Fig. 5), contributing to the overall signal.

### 4. Time-dependent and regional correlations of angular momentum and polar motion

When the total correlation between atmospheric and geodetic excitation functions for polar motion is performed in a time dependent manner, we note that the correlations have increased since the 1960s. After about 1984, the correlation in quarter-year intervals is significant at the 99% level (greater than 0.33; Nastula & Salstein 1999a), so that we have confidence in using the polar motion and atmospheric data for this purpose.

Time-variable spectra of the  $\chi$  vector reveal that signals centered around 50 days and those between 75 and 125 days are dominant. The geographical source for much of the variability resides in the land areas of the Northern Hemisphere, primarily northern Eurasia and North America (Nastula & Salstein 1999a). The special importance of Eurasia becomes particularly evident when modes of variability in the atmosphere are also investigated (Nastula & Salstein

1999b). Atmospheric modes may be determined empirically; in such cases the first mode contains the greatest variance in the time series. A second method of examining atmospheric modes is to find the contribution of an important region (like the Eurasian region) to patterns that have been determined from other studies of the atmosphere (*e.g.* Wallace & Gutzler 1983; Lau *et al.* 1994). In this case the modes known as El Niño, the North Atlantic Oscillation and the North Atlantic/Eurasia modes have a strong contribution for polar motion forcing from the northern Eurasian region.

## 5. Influence of the oceans on polar motion

When the influence of an ocean model is added to that of the atmosphere (*e.g.* Ponte & Stammer 1999) there tends to be a reduction in variance when the difference between the geophysical fluid forcing and the geodetic response is studied. Thus Fig. 6 shows the contribution of excitation fields from the ocean model, the atmospheric analyses and the sum of the two as compared with geodetic polar motion forcing, for one sample component,  $\chi_2$  ( $\chi_1$  shows similar results). Here it is clear that there are times when the atmosphere is particularly important in the polar motion signal and other occasions when the ocean is important. When the contribution from the two are summed, the amount of variance explained by atmosphere and ocean is less than that of either alone, as Table 2 shows (Ponte & Stammer 1999). For more details, see Nastula *et al.* (this volume).

Table 2. Percentage of variance in excitation of polar motion explained by ocean and atmosphere (courtesy, R. Ponte).

Ocean	Atmosphere	Ocean + Atmosphere
$\chi_1$ 30%	6%	53%
$\chi_2$ -44%	43%	73%

## 6. Forecasts of polar motion excitation terms

As part of the mission of the Special Bureau for the Atmosphere of the IERS, forecasts of excitation terms are performed by advancing the equations of motion of the atmosphere. These dynamical forecasts are performed with lead times out to those given in Table 1. To estimate the usefulness of such forecasts, we compare the difference between forecasted value and analyzed value based on both these dynamic forecasts and a statistical competitor. Though more complicated statistical forecasts can be considered as competitors (Rosen *et al.* 1991) we chose a “persistence-based” forecast, namely, one for which the state of the atmosphere remains fixed. The daily values of the dynamic and persistence-based forecast given for the one-day lead time, as an example, for 1992 show

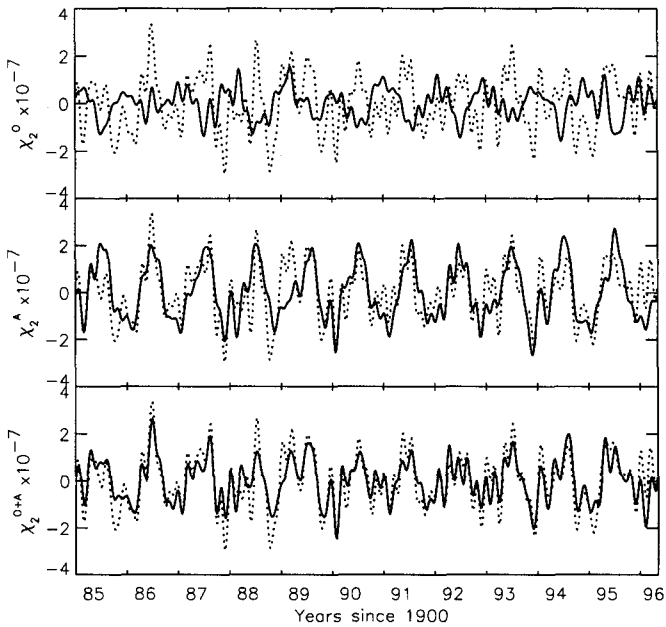


Figure 6. Comparison of geodetic excitation term (dashed, all panels), with the atmospheric excitation term (solid, top panel), with the ocean term (solid, middle), and with the atmosphere plus ocean (bottom), all filtered between 3.7 years and 60 days.

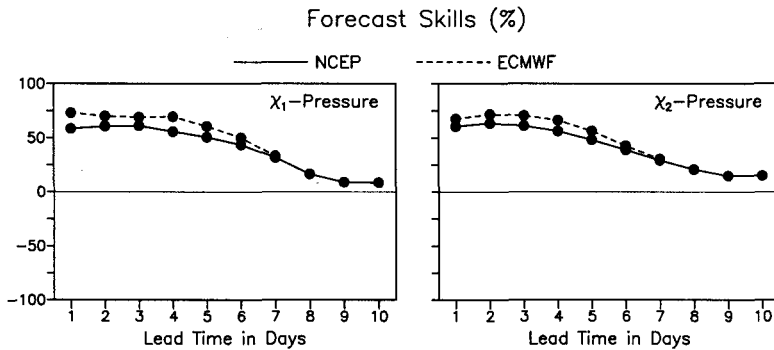


Figure 7. Forecast skills in percent of the two atmospheric excitation terms with lead times up to 10 days for the U.S. National Centers for Environmental Prediction and the European Center for Medium Range Weather Forecasts for 1992.

variance that is considerably smaller in the dynamic forecast. The skill,  $S$ , of such a forecast, defined below, will be greater than 0 for the forecast to be useful.

$$S = [(\varepsilon_{per} - \varepsilon_{dyn}) / \varepsilon_{per}] \times 100\%.$$

Here  $\varepsilon_{per}$  and  $\varepsilon_{dyn}$  are the root mean squared error of the dynamic and persistence forecasts. Skills for  $\chi_1$  and  $\chi_2$  from two meteorological centers are plotted in Fig. 7 for two series during a year in which such data, 1992, were available with a long lead time. We note that the skill is positive for all the available lead times, out to 10 days. Skills between 1 and 4 days are over 50%.

### 7. APPENDIX — Availability of the SBA data

Effective angular momentum functions, including those for polar motion from the four operational analyses and from the NCEP/NCAR reanalysis system are currently available from the AER Web page at:

<http://www.aer.com/groups/diag/sb.html>. The variables are also available in near-real time, in both analysis and forecast form, for at least the past 10 days, by anonymous ftp from the NCEP server at <ftp.ncep.noaa.gov> under subdirectory [pub/cpc/long/aam](ftp.ncep.noaa.gov/pub/cpc/long/aam). Further details of the data availability are given in Salstein & Miller (1999).

**Acknowledgments.** The work was funded under the U.S. NASA's Earth Observing System Program, NAS5-6309. I thank Peter Nelson of AER and A. J. Miller of NCEP for helping in the production of the SBA data sets. Rui Ponte of AER supplied the ocean model results, and Jolanta Nastula of the Space Research Center, Warsaw, Poland, helped with the regional analysis of polar motion. The International Astronomical Union supported my travel to the symposium, and I thank the local organizing committee in Cagliari for their arrangements and hospitality.

## References

- Barnes, R.T., H.R. Hide, A.A. White & C.A. Wilson, 1983, Atmospheric angular momentum fluctuations, length-of-day changes and polar motion. *Proc. Roy. Soc. London, Ser. A.*, **387**, 31–73.
- Bell, M.J., 1994, Oscillations in the equatorial component of the atmospheres angular momentum and torques on the earth's bulge. *Q. J. Meteorol. Soc.*, **120**, 195–213.
- Hsu, H.H. & B.J. Hoskins, 1989, Tidal fluctuations as seen in ECMWF data. *Q. J. Meteorol. Soc.*, **115**, 247–264.
- Lau, W.K., P.J. Sheu & I.S. Kang, 1994, Multi-scale low frequency circulation modes in the global atmosphere. *J. Atmos. Sci.*, **51**, 1169–1193.
- Nastula, J. & D.A. Salstein, 1999a, Regional atmospheric angular momentum contributions to polar motion excitation, *J. Geophys. Res.*, **104**, 7347–7358.
- Nastula, J. & D.A. Salstein, 1999b, Atmospheric forcing of polar motion and climate patterns. Abstract, International Union of Geodesy and Geophysics 1999 Congress, Birmingham, UK.
- Ponte, R.M. & P. Gaspar, 1999, Regional analysis of the inverted barometer over the global ocean using TOPEX/Poseidon data and model results, *J. Geophys. Res.*, **104**, 15587–15601.
- Ponte, R.M. & D. Stammer, 1999, Role of ocean currents and bottom pressure variability on seasonal polar motion. *J. Geophys. Res.*, **104**, 23393–23409.
- Rosen, R.D., D.A. Salstein & T. Nehr Korn, 1991, Predictions of zonal wind and angular momentum by the NMC medium-range forecast model during 1985–89. *Mon. Wea. Rev.*, **119**, 208–217.
- Salstein, D.A., D.M. Kann, A.J. Miller & R.D. Rosen, 1993, The sub-bureau for atmospheric angular momentum of the International Earth Rotation Service, A Meteorological data center with geodetic applications. *Bull. Amer. Meteor. Soc.*, **74**, 67–80.
- Salstein, D. & A.J. Miller, 1999, Special Bureau for the Atmosphere, to appear in Technical Note 28, Mission of the GGF Center, International Earth Rotation Service, Paris, France. Ben Chao, editor.
- Wallace, J.M. & D.S. Gutzler, 1981, Teleconnections in the geopotential height field during the Northern Hemisphere winter. *Mon. Wea. Rev.*, **104**, 784–812.